

UC San Diego

UC San Diego Previously Published Works

Title

Dynamic behaviour of the East Antarctic ice sheet during Pliocene warmth

Permalink

<https://escholarship.org/uc/item/7cq9w66z>

Journal

Nature Geoscience, 6(9)

ISSN

1752-0894

Authors

Cook, CP
Van De Flierdt, T
Williams, T
et al.

Publication Date

2013

DOI

10.1038/ngeo1889

Peer reviewed

Dynamic behaviour of the East Antarctic ice sheet during Pliocene warmth

Carys P. Cook^{1,2*}, Tina van de Flierdt², Trevor Williams³, Sidney R. Hemming^{3,4}, Masao Iwai⁵, Munemasa Kobayashi⁵, Francisco J. Jimenez-Espejo^{6,7}, Carlota Escutia⁷, Jhon Jairo González⁷, Boo-Keun Khim⁸, Robert M. McKay⁹, Sandra Passchier¹⁰, Steven M. Bohaty¹¹, Christina R. Riesselman^{12,13}, Lisa Tauxe¹⁴, Saiko Sugisaki^{14,15}, Alberto Lopez Galindo⁷, Molly O. Patterson⁹, Francesca Sangiorgi¹⁶, Elizabeth L. Pierce¹⁷, Henk Brinkhuis¹⁶ and IODP Expedition 318 Scientists[†]

Warm intervals within the Pliocene epoch (5.33–2.58 million years ago) were characterized by global temperatures comparable to those predicted for the end of this century¹ and atmospheric CO₂ concentrations similar to today^{2–4}. Estimates for global sea level highstands during these times⁵ imply possible retreat of the East Antarctic ice sheet, but ice-proximal evidence from the Antarctic margin is scarce. Here we present new data from Pliocene marine sediments recovered offshore of Adélie Land, East Antarctica, that reveal dynamic behaviour of the East Antarctic ice sheet in the vicinity of the low-lying Wilkes Subglacial Basin during times of past climatic warmth. Sedimentary sequences deposited between 5.3 and 3.3 million years ago indicate increases in Southern Ocean surface water productivity, associated with elevated circum-Antarctic temperatures. The geochemical provenance of detrital material deposited during these warm intervals suggests active erosion of continental bedrock from within the Wilkes Subglacial Basin, an area today buried beneath the East Antarctic ice sheet. We interpret this erosion to be associated with retreat of the ice sheet margin several hundreds of kilometres inland and conclude that the East Antarctic ice sheet was sensitive to climatic warmth during the Pliocene.

Recent satellite observations reveal that the Greenland and West Antarctic ice sheets are losing mass in response to climatic warming⁶. Basal melting of ice shelves by warmer ocean temperatures is proposed as one of the key mechanisms facilitating mass loss of the marine-based West Antarctic ice sheet⁷. Although thinning of ice shelves and acceleration of glaciers has been described

for some areas of the East Antarctic margin⁷, the mass balance of the predominantly land-based East Antarctic ice sheet is less clear⁸. Its vulnerability to warmer-than-present temperatures may be particularly significant in low-lying regions, such as the Wilkes Subglacial Basin (Fig. 1).

This hypothesis can be tested by studying intervals from geological records deposited under similar environmental conditions to those predicted for the near future. Warm intervals within the Pliocene epoch are such analogues, with mean annual global temperatures between 2 and 3 °C higher than today¹ and atmospheric CO₂ concentrations between 350 and 450 ppm, 25–60% higher than pre-industrial values^{2–4}. Estimates for eustatic sea level highstands during these times, reconstructed from benthic foraminiferal oxygen isotopes⁵ and palaeoshoreline reconstructions⁹, are variable but indicate 22 ± 10 m of sea level rise, although estimates derived from palaeoshoreline reconstructions may need corrections for glacio-isostatic adjustments¹⁰. Complete melting of Greenland and West Antarctica's ice sheets could account for around 12 m (ref. 11) of eustatic sea level rise, indicating that most estimates for Pliocene sea level require a contribution from the East Antarctic ice sheet. Although ice sheet modelling suggests that low-lying areas of the East Antarctic continent may be candidates for Pliocene ice sheet loss^{12,13}, direct evidence from ice-proximal records on locations of ice margin retreat are limited^{14–16}.

To improve our understanding of the response of the East Antarctica ice sheet to past warm climates, Integrated Ocean Drilling Program Site U1361 (64° 24' 5" S 143° 53' 1" E; 3,465 m water depth) was drilled during Expedition 318 into a submarine

¹The Grantham Institute for Climate Change, Imperial College London, South Kensington Campus, Prince Consort Road, London SW7 2AZ, UK,

²Department of Earth Science and Engineering, Imperial College London, South Kensington Campus, Prince Consort Road, London SW7 2AZ, UK, ³Lamont Doherty Earth Observatory of Columbia University, PO Box 1000, 61 Route 9W, Palisades, New York 10964, USA, ⁴Department of Earth and Environmental Sciences, Columbia University, New York 10027, USA, ⁵Department of Natural Science, Kochi University, 2-5-1 Akebono-cho, Kochi 780-8520, Japan, ⁶Department of Earth and Planetary Sciences, Graduate School of Environmental Studies, Nagoya University, D2-2 (510), Furo-cho, Chikusa-ku, Nagoya 464-8601, Japan, ⁷Instituto Andaluz de Ciencias de la Tierra, CSIC-UGR, 18100 Armilla, Spain, ⁸Department of Oceanography, Pusan National University, Busan 609-735, Republic of Korea, ⁹Antarctic Research Centre, Victoria University of Wellington, PO Box 600, Wellington 6140, New Zealand, ¹⁰Earth and Environmental Studies, Montclair State University, 252 Mallory Hall, 1 Normal Avenue, Montclair, New Jersey 07043, USA, ¹¹Ocean and Earth Science, National Oceanography Centre Southampton, University of Southampton, European Way, SO14 3ZH, Southampton, UK, ¹²Department of Geology, University of Otago, PO Box 56, Dunedin 9054, New Zealand, ¹³Department of Marine Science, University of Otago, PO Box 56, Dunedin 9054, New Zealand, ¹⁴Scripps Institution of Oceanography, University of California, San Diego, La Jolla, California 92093-0220, USA, ¹⁵Department of Earth and Planetary Sciences, University of Tokyo, 7-3-1 Hongo, Bunkyo-ku, Tokyo 113-0033, Japan, ¹⁶Department of Earth Sciences, Faculty of Geosciences, Utrecht University, Laboratory of Palaeobotany and Palynology, Budapestlaan 4, 3584CD, Utrecht, The Netherlands, ¹⁷Department of Geosciences, Wellesley College, 106 Central Street, Wellesley, Massachusetts 02481, USA, [†]A full list of authors and their affiliations appears at the end of the paper.

*e-mail: c.cook09@imperial.ac.uk

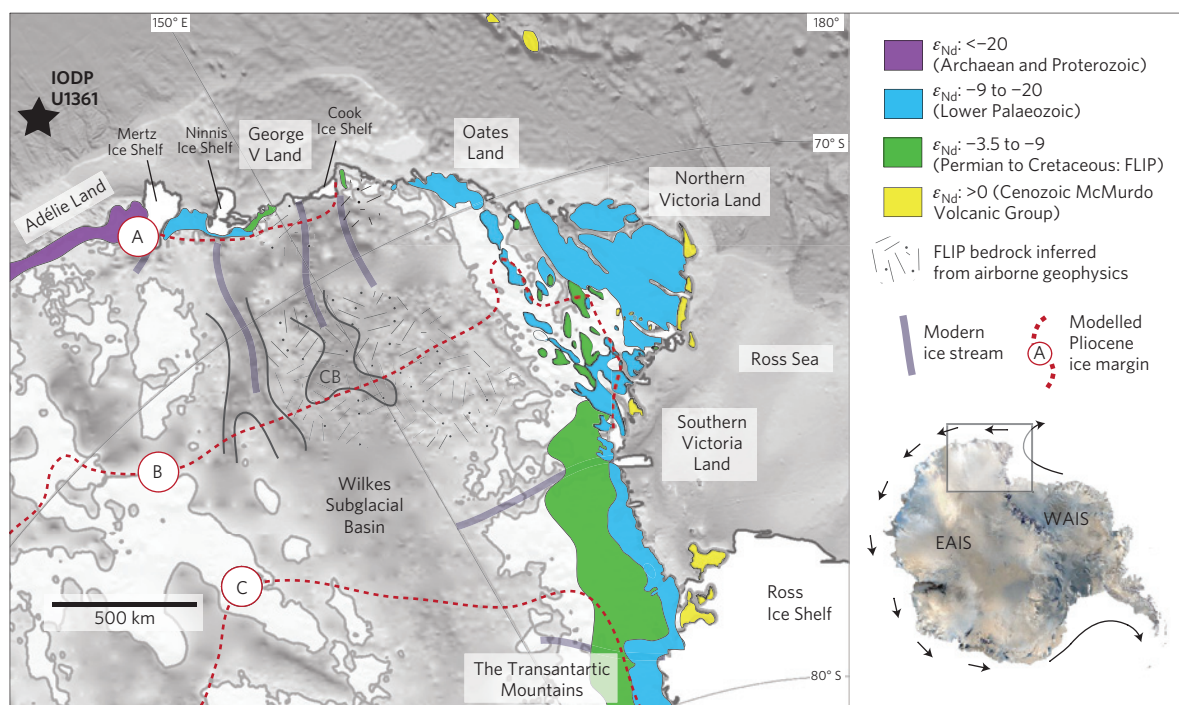


Figure 1 | Regional map of study area, including geology of outcrops and inferred subglacial geology. Coloured shading represents the simplified geographical extent of four geological terranes differentiated according to their neodymium isotopic characteristics (expressed as ϵ_{Nd} ; see Supplementary Section S1 for detailed geological context). Areas above sea level are shown in pale grey with grey outlines, and ice shelves are shown in white²⁴. Outline of the Central Basin (CB) denotes its location within the Wilkes Subglacial Basin²³. Red lines denote the spatial extent of modelled maximum East Antarctic ice sheet retreat for the Pliocene: line A, 3 m (ref. 28), line B, 10 m (ref. 12), line C, 16 m (ref. 13). The inset map illustrates the westward-flowing Antarctic coastal current (arrows). EAIS, East Antarctic ice sheet; WAIS, West Antarctic ice sheet.

levee bank, 310 km offshore of the Adélie Land margin, East Antarctica (Fig. 1). Approximately 75 m of continuous Pliocene marine sediments, within the resolution of available biostratigraphic and magnetostratigraphic data¹⁷, were recovered. Available physical property¹⁸, sedimentology¹⁸, and palaeomagnetic and micropalaeontology data¹⁷ are here combined with new opal (%) data, bulk geochemistry data, and radiogenic isotope data from analyses of detrital sediments.

The Pliocene study section at IODP Site U1361 spans an interval between 5.3 and 3.3 Myr ago and contains a sedimentary sequence alternating between eight diatom-rich silty clay layers, and eight diatom-poor clay layers with silt laminations (Fig. 2). Diatom-rich sediments have higher diatom valve and bulk-sediment biogenic opal concentrations, and distinctively lower signals in natural gamma radiation (Fig. 2), indicating lower clay content. The diatom-rich units are also characterized by higher Ba/Al ratios (Fig. 2), pointing to multiple extended periods of increased biological productivity related to less sea ice, and warmer spring and summer sea surface temperatures. This inference is supported by diatom and silicoflagellate assemblage and TEX₈₆ palaeothermometry data from marine and land-based records from the Antarctic Peninsula margin¹⁹, the Kerguelen Plateau²⁰, Prydz Bay^{15,16,19,21} and the Ross Sea²². These reconstructions identify elevated mean annual Pliocene sea surface temperatures^{15,19–21}, spring and summer sea surface temperatures between 2 and 6 °C above modern levels^{19,22}, and prolonged warm intervals spanning up to 200,000 years in duration, superimposed on a baseline of warmer-than-present temperatures.

To constrain the effects of prolonged warming on the dynamics of the East Antarctic ice sheet, we produced a Pliocene record of continental erosion patterns based on detrital marine sediment provenance (<63 μm grain-size fraction) from IODP Site U1361. We used the radiogenic isotope compositions of neodymium

(¹⁴³Nd/¹⁴⁴Nd, expressed as ϵ_{Nd} , which describes the deviation of measured ¹⁴³Nd/¹⁴⁴Nd ratios from the Chondritic Uniform Reservoir in parts per 10,000) and strontium (⁸⁷Sr/⁸⁶Sr), both of which vary in continental rocks on the basis of the age and lithology of geological terranes. In IODP Site U1361 sediments, both ratios show significant variations throughout the studied Pliocene interval, with ϵ_{Nd} values ranging from -5.9 to -14.7 and Sr isotopic compositions from 0.712 to 0.738 (Fig. 2). Notably, both ratios co-vary in a distinct pattern that parallels lithological units, physical properties and bulk sediment geochemistry (Fig. 2), with a more radiogenic Nd isotopic composition and a less radiogenic Sr isotopic composition characteristic of sediments deposited during periods of Pliocene warmth (ϵ_{Nd} : -5.9 to -9.5; ⁸⁷Sr/⁸⁶Sr: 0.712–0.719; Figs 2–3).

East Antarctic continental geological terranes in the vicinity of IODP Site U1361 encompass a diverse range of lithologies and ages: Archaean to Proterozoic basement along the adjacent Adélie Land coast; Lower Palaeozoic bedrock in the vicinity of the nearby Ninnis and Mertz glaciers, along the Oates Land coast, in Northern and Southern Victoria Land, and in the Transantarctic Mountains; Jurassic to Cretaceous volcanic rocks (the Ferrar Large Igneous Province (FLIP) and associated sedimentary rocks of the Beacon Supergroup) along the George V Land coast, in Northern and Southern Victoria Land, and in the Transantarctic Mountains; and Cenozoic volcanics of the McMurdo Volcanic Group. Each of these terranes can be characterized in Nd–Sr isotope space (Fig. 3). The provenance signatures of the two Pliocene sedimentary types at IODP Site U1361 (that is, diatom-rich and diatom-poor) can be best explained by a mixture of FLIP bedrock (ϵ_{Nd} : -3.5 to -6.9; ⁸⁷Sr/⁸⁶Sr: 0.709–0.719), and lower Palaeozoic bedrock (ϵ_{Nd} : -11.2 to -19.8; ⁸⁷Sr/⁸⁶Sr: 0.714–0.753; Fig. 1) (Fig. 3; see Supplementary Section S1 for further details on local geology and potential endmembers).

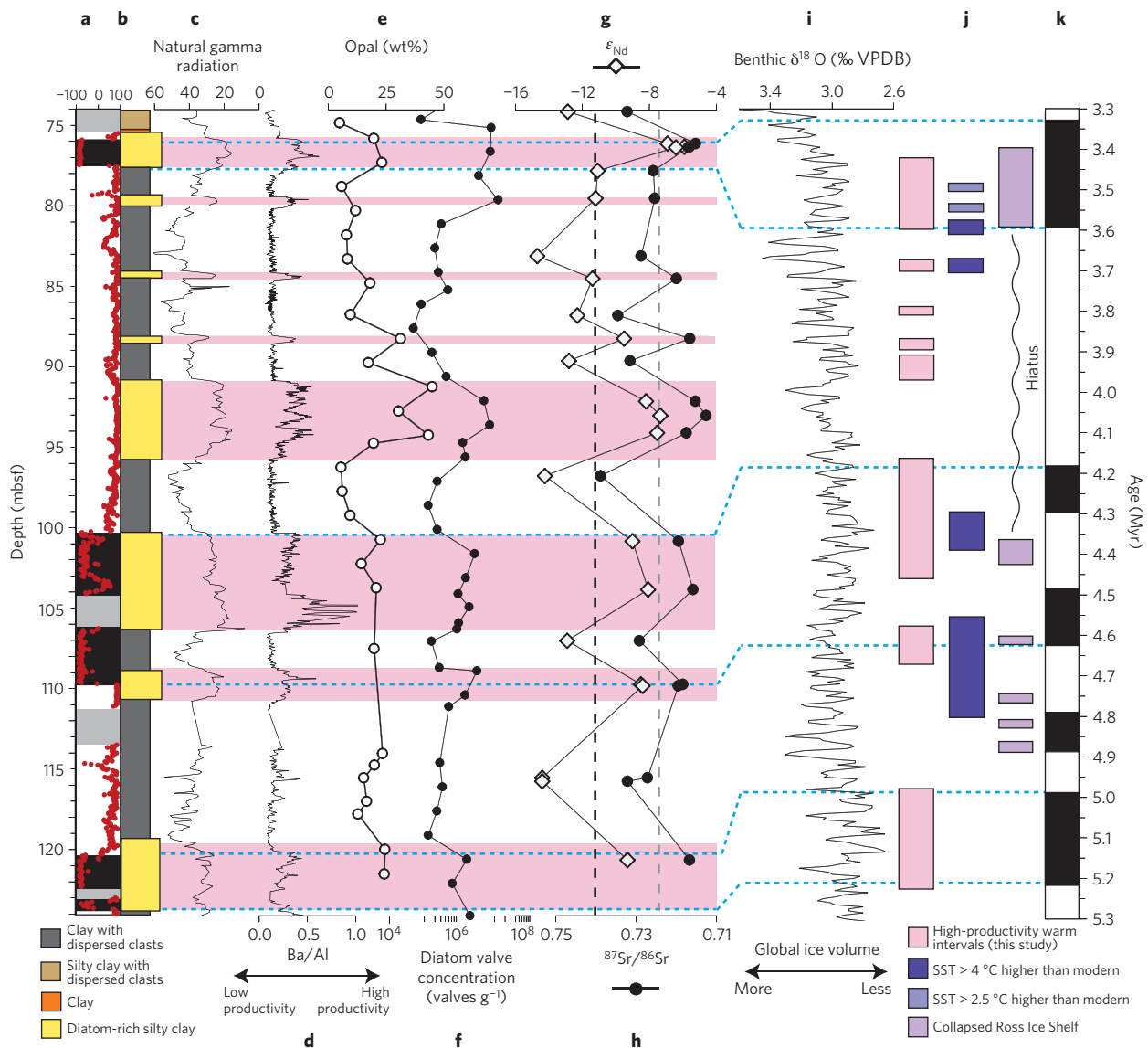


Figure 2 | Pliocene records from IODP Site U1361 in comparison to other circum-Antarctic and global records. **a**, Palaeomagnetic chron boundaries based on inclination measurements¹⁷ (red data points); grey shading indicates intervals with no data. **b**, Lithostratigraphy¹⁸. **c–h**, Expedition 318 shipboard record of natural gamma radiation, and new records of Ba/Al, opal wt%, diatom valve concentrations, and Nd and Sr isotopic compositions; pink shading, high-productivity intervals based on natural gamma radiation; vertical black stippled lines, Holocene Nd and Sr isotopic compositions (core-tops). **i**, Global benthic oxygen isotope stack (LR04; ref. 29). **j**, Circum-Antarctic indicators for warm temperatures; pink, Pliocene high-productivity intervals at IODP Site U1361; dark blue, diatom and silicoflagellate assemblages from the Kerguelen Plateau²⁰ and Prydz Bay¹⁹; light blue, silicoflagellate assemblages from Prydz Bay²¹; lilac, diatomite deposits from ANDRILL cores in the Ross Sea²⁵. **k**, Palaeomagnetic timescale³⁰.

Diatom-poor sediments have a provenance signature that matches lower Palaeozoic bedrock, most likely sourced from granitic bedrock in the hinterland of the nearby Ninnis Glacier (Fig. 1). In contrast, the provenance fingerprint of sediments deposited during warm Pliocene intervals (diatom-rich units) reveals that they are predominantly composed of FLIP material. This FLIP provenance fingerprint is not found in Holocene deposits at IODP Site U1361 or in sediments in its vicinity, and seems to be unique to diatom-rich Pliocene marine sediments over the past 5.3 Myr (Fig. 3 and Supplementary Section S1).

We suggest that the most likely source of eroded FLIP material is the Wilkes Subglacial Basin, which requires Pliocene retreat of the East Antarctic ice sheet. Aeromagnetic data collected over the Wilkes Subglacial Basin between $\sim 70^\circ\text{S}$ and 74°S (ref. 23) reveal anomalies that resemble exposed FLIP bedrock in Southern Victoria Land, indicating the presence of abundant

intrusive sills, as well as two large approximately 2-kilometre-deep graben-like sub-basins²³ (Fig. 1). Recent subglacial topographic data compilations²⁴ furthermore demonstrate that these sub-basins are directly connected to the Southern Ocean below sea level, and aerogeophysical data suggest that the Central Basin contains unconsolidated sediments inferred to be FLIP in origin²³ (Fig. 1).

We propose that enhanced erosion of FLIP material in the Central Basin was achieved by multiple retreats of the ice margin. Ice sheet modelling and modern observations suggest that sub-surface melting at the ice edge in response to warm ocean temperatures drives retreat in areas where grounding lines lie below sea level⁷, such as the mouth of the Wilkes Subglacial Basin²⁴ (Supplementary Section S1). Warm Pliocene ocean waters would have facilitated retreat into the Central Basin, contemporaneous with ice shelf collapse and ice margin retreat in other circum-Antarctic locations, such as in the Prydz Bay area^{15,16} and the Ross Sea²⁵.

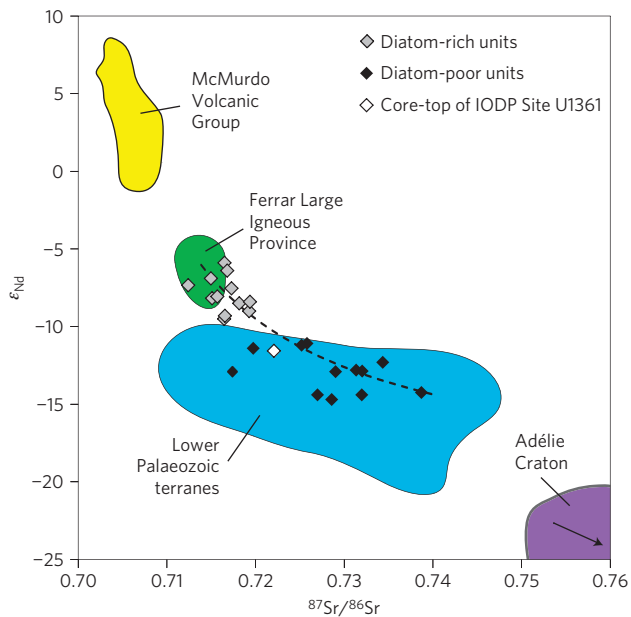


Figure 3 | Neodymium and strontium isotopic composition of Pliocene detrital sediments from IODP Site U1361 and East Antarctic geological terranes proximal to the study area. Fields for the isotopic composition of various terranes are based on literature values (see Supplementary Section S1). Data corresponding to the Adélie Land Craton primarily plot outside the neodymium and strontium isotopic space shown (ϵ_{Nd} : -20 to -28 ; $^{87}\text{Sr}/^{86}\text{Sr}$: 0.750 – 0.780).

Zones of maximum glacial erosion are typically associated with the margins of an ice sheet^{26,27}, suggesting that the retreated Pliocene ice margin was situated on FLIP bedrock within the Central Basin. Existing ice sheet models imply that between ~ 3 m (ref. 28; line A, Fig. 1) and ~ 16 m (ref. 13; line C, Fig. 1) of Pliocene glacio-eustatic sea level rise could be derived from retreat of the East Antarctic ice sheet. The smallest estimate (3 m) is unlikely to accurately represent the response of the ice margin to the warmest range of Pliocene climate conditions²⁸, and larger estimates (10–16 m; refs 12,13) are probably influenced by initial ice sheet configurations used within climate modelling frameworks. Our new data, as well as maximum modelled erosion for the northern part of the Wilkes Subglacial Basin²⁷ are in agreement with retreat of the ice margin several hundred kilometres inland. Such retreat could have contributed between 3 and 10 m of global sea level rise from the East Antarctic ice sheet, providing a new and crucial target for future ice sheet modelling. Irrespective of the extent of ice retreat, our data document a dynamic response of the East Antarctic ice sheet to varying Pliocene climatic conditions, revealing that low-lying areas of Antarctica's ice sheets are vulnerable to change under warmer-than-modern conditions, with important implications for the future behaviour and sensitivity of the East Antarctic ice sheet.

Received 18 January 2013; accepted 17 June 2013;
published online 21 July 2013

References

- Haywood, A. M. & Valdes, P. J. Modelling Pliocene warmth: Contribution of atmosphere, oceans and cryosphere. *Earth Planet. Sci. Lett.* **218**, 363–377 (2004).
- Seki, O. *et al.* Alkenone and boron-based Pliocene p_{CO_2} records. *Earth Planet. Sci. Lett.* **292**, 201–211 (2010).
- Bartoli, G., Honisch, B. & Zeebe, R. E. Atmospheric p_{CO_2} decline during the Pliocene intensification of Northern Hemisphere glaciations. *Paleoceanography* **26**, PA4213 (2011).
- Pagani, M., Liu, Z. H., LaRiviere, J. & Ravelo, A. C. High Earth-system climate sensitivity determined from Pliocene carbon dioxide concentrations. *Nature Geosci.* **3**, 27–30 (2010).

- Miller, K. G. *et al.* High tide of the warm Pliocene: Implications of global sea level for Antarctic deglaciation. *Geology* **40**, 407–410 (2012).
- Rignot, E., Velicogna, I., van den Broeke, M. R., Monaghan, A. & Lenaerts, J. Acceleration of the contribution of the Greenland and Antarctic ice sheets to sea level rise. *Geophys. Res. Lett.* **38**, L05503 (2011).
- Pritchard, H. D. *et al.* Antarctic ice-sheet loss driven by basal melting of ice shelves. *Nature* **484**, 502–505 (2012).
- Shepherd, A. *et al.* A reconciled estimate of ice-sheet mass balance. *Science* **338**, 1183–1189 (2012).
- Naish, T. R. & Wilson, G. S. Constraints on the amplitude of Mid-Pliocene (3.6–2.4 Ma) eustatic sea-level fluctuations from the New Zealand shallow-marine sediment record. *Phil. Trans. R. Soc. A* **367**, 169–187 (2009).
- Raymo, M. E., Mitrovica, J. X., O'Leary, M. J., DeConto, R. M. & Hearty, P. L. Departures from eustasy in Pliocene sea-level records. *Nature Geosci.* **4**, 328–332 (2011).
- Lythe, M. B., Vaughan, D. G. & Consortium, B. BEDMAP: A new ice thickness and subglacial topographic model of Antarctica. *J. Geophys. Res.* **106**, 11335–11351 (2001).
- Hill, D. J., Haywood, A. M., Hindmarsh, R. C. A. & Valdes, P. J. in *Deep Time Perspectives on Climate Change* (eds Williams, M., Haywood, A.M., Gregory, J. & Schmidt, D.) 517–538 (The Micropalaeontological Society/The Geological Society of London, 2007).
- Dolan, A. M. *et al.* Sensitivity of Pliocene ice sheets to orbital forcing. *Paleogeogr. Paleoclimatol. Paleoecol.* **309**, 98–110 (2011).
- Williams, T. *et al.* Evidence for iceberg armadas from East Antarctica in the Southern Ocean during the late Miocene and early Pliocene. *Earth Planet. Sci. Lett.* **290**, 351–361 (2010).
- Whitehead, J. M., Quilty, P. G., Harwood, D. M. & McMinn, A. Early Pliocene paleoenvironment of the Sørsdal Formation, Vestfold Hills, based on diatom data. *Mar. Micropaleontol.* **41**, 125–152 (2001).
- Whitehead, J. M. & McKelvey, B. C. The stratigraphy of the Pliocene-lower Pleistocene Bardin Bluffs Formation, Amery Oasis, northern Prince Charles Mountains, Antarctica. *Antarctic Sci.* **13**, 79–86 (2001).
- Tauxe, L. *et al.* Chronostratigraphic framework for the IODP Expedition 318 cores from the Wilkes Land Margin: Constraints for paleoceanographic reconstruction. *Paleoceanography* **27**, PA2214 (2012).
- Escutia, C., Brinkhuis, H., Klaus, A. & Expedition 318 Scientists, *Proc. Integrated Ocean Drilling Program Vol. 318* (Integrated Ocean Drilling Program Management International, 2011).
- Escutia, C. *et al.* Circum-Antarctic warming events between 4 and 3.5 Ma recorded in marine sediments from the Prydz Bay (ODP Leg 188) and the Antarctic Peninsula (ODP Leg 178) margins. *Glob. Planet. Change* **69**, 170–184 (2009).
- Bohaty, S. M. & Harwood, D. M. Southern Ocean Pliocene paleotemperature variation from high-resolution silicoflagellate biostratigraphy. *Mar. Micropaleontol.* **33**, 241–272 (1998).
- Whitehead, J. M. & Bohaty, S. M. Pliocene summer sea surface temperature reconstruction using silicoflagellates from Southern Ocean ODP Site 1165. *Paleoceanography* **18**, 1075 (2003).
- McKay, R. M. *et al.* Antarctic and Southern Ocean influences on Late Pliocene global cooling. *Proc. Natl Acad. Sci. USA* **109**, 6423–6428 (2012).
- Ferraccioli, F., Armadillo, E., Jordan, T., Bozzo, E. & Corr, H. Aeromagnetic exploration over the East Antarctic Ice Sheet: A new view of the Wilkes Subglacial Basin. *Tectonophysics* **478**, 62–77 (2009).
- Fretwell, P. *et al.* Bedmap2: Improved ice bed, surface and thickness datasets for Antarctica. *Cryosphere* **7**, 375–393 (2013).
- Naish, T. *et al.* Obliquity-paced Pliocene West Antarctic ice sheet oscillations. *Nature* **458**, 322–328 (2009).
- Alley, R. B. *et al.* How glaciers entrain and transport basal sediment: Physical constraints. *Quat. Sci. Rev.* **16**, 1017–1038 (1997).
- Jamieson, S. S. R., Sugden, D. E. & Hulton, N. R. J. The evolution of the subglacial landscape of Antarctica. *Earth Planet. Sci. Lett.* **293**, 1–27 (2010).
- Pollard, D. & DeConto, R. M. Modelling West Antarctic ice sheet growth and collapse through the past five million years. *Nature* **458**, 329–332 (2009).
- Lisiecki, L. E. & Raymo, M. E. A Pliocene-Pleistocene stack of 57 globally distributed benthic $\delta^{18}\text{O}$ records. *Paleoceanography* **20**, PA1003 (2005).
- Gradstein, F., Ogg, J., Schmitz, M. & Ogg, G. *The Geological Time Scale* (Elsevier, 2012).

Acknowledgements

This research used samples and data provided by the Integrated Ocean Drilling Program (IODP). The IODP is sponsored by the US National Science Foundation (NSF) and participating countries under the management of Joint Oceanographic Institutions. We thank B. Coles and K. Kreissig for technical laboratory support, and A. G. C. Graham for assistance with cartography. Financial support for this study was provided by NERC UK IODP to T.v.d.F. (grants NE/H014144/1 and NE/H025162/1), by the European Commission to T.v.d.F. (grant IRG 230828), by the National Science Foundation to T.W., T.v.d.F. and S.R.H. (grant ANT 09-44489), by the NSF to S.P. (grant OCE 1060080), by the Spanish Ministry of Science and Innovation to C.E. (grant CTM

2011-24079), by the National Science Foundation to L.T. (grant OCE 1058858), by the Netherlands Organisation for Scientific Research to F.S. and H.B. (grant 86610110), by the Japanese Society for the Promotion of Science KAKHANI to M.I. (grants 25550015 and 23244102) and by the National Research Foundation of Korea to B-K.K. (grant 2011-0021632).

Author contributions

C.P.C., T.v.d.F., T.W. and S.R.H. designed the research; C.P.C. carried out the neodymium and strontium isotope analyses; M.I. and M.K. performed the diatom counts, interpreted in discussion with S.M.B. and C.R.R.; F.J.J.-E., J.J.G. and C.E. were responsible for XRF bulk geochemistry analyses; R.M.M., M.O.P. and S.P. carried out sedimentological analyses; A.L.G., F.J.J.-E. and C.E. collected clay mineralogy data;

B-K.K. analysed opal contents; L.T. and S.S. were responsible for magnetic analyses. All authors contributed to the interpretation of the data. C.P.C. and T.v.d.F. wrote the paper with input from all authors.

Additional information

Supplementary information is available in the [online version of the paper](#). Reprints and permissions information is available online at www.nature.com/reprints. Correspondence and requests for materials should be addressed to C.P.C.

Competing financial interests

The authors declare no competing financial interests.

Adam Klaus¹⁸, Annick Fehr¹⁹, James A. P. Bendle²⁰, Peter K. Bijl²¹, Stephanie A. Carr²², Robert B. Dunbar²³, José Abel Flores²⁴, Travis G. Hayden²⁵, Kota Katsuki²⁶, Gee Soo Kong²⁷, Mutsumi Nakai²⁸, Matthew P. Olney²⁹, Stephen F. Pekar³⁰, Jörg Pross³¹, Ursula Röhl³², Toyosaburo Sakai³³, Prakash K. Shrivastava³⁴, Catherine E. Stickley³⁵, Shouting Tuo³⁶, Kevin Welsh³⁷ and Masako Yamane³⁸

¹⁸United States Implementing Organization, Integrated Ocean Drilling Program, Texas A&M University, 1000 Discovery Drive, College Station, Texas 77845, USA, ¹⁹RWTH Aachen University, Institute for Applied Geophysics and Geothermal Energy, Mathieustrasse 6, D-52074 Aachen, Germany, ²⁰School of Geographical, Earth and Environmental Sciences, Aston Webb Building, University of Birmingham, Edgbaston, B15 2TT, UK, ²¹Department of Earth Sciences, Faculty of Geosciences, Utrecht University, Laboratory of Palaeobotany and Palynology, Budapestlaan 4, 3584CD, Utrecht, The Netherlands, ²²Department of Chemistry and Geochemistry, Colorado School of Mines, 1500 Illinois Street, Golden, Colorado 80401, USA, ²³Environmental Earth System Science, Stanford University, Stanford, California 94305-2115, USA, ²⁴Department of Geology, Universidad de Salamanca, 37008, Salamanca, Spain, ²⁵Department of Geology, Western Michigan University, 1187 Rood Hall, 1903 West Michigan Avenue, Kalamazoo, Michigan 49008, USA, ²⁶Geological Research Division, Korea Institute of Geoscience and Mineral Resources, 124 Gwahang-no, Yuseong-gu, Daejeon 305-350, Korea, ²⁷Petroleum and Marine Research Division, Korea Institute of Geoscience and Mineral Resources, 30 Gajeong-dong, Yuseong-gu, Daejeon 305-350, Korea, ²⁸Education Department, Daito Bunka University, 1-9-1 Takashima-daira, Itabashi-ku, Tokyo 175-8571, Japan, ²⁹Department of Geology, University of South Florida, Tampa, 4202 East Fowler Avenue, SCA 528, Tampa, Florida 33620, USA, ³⁰School of Earth and Environmental Sciences, Queens College, 65-30 Kissena Boulevard, Flushing, New York 11367, USA, ³¹Paleoenvironmental Dynamics Group, Institute of Geosciences, Goethe-University Frankfurt, Altenhö ferallee 1, 60438 Frankfurt, Germany, ³²MARUM—Center for Marine Environmental Sciences, University of Bremen, Leobener Straße, 28359 Bremen, Germany, ³³Department of Geology, Utsunomiya University, 350 Mine-Machi, Utsunomiya 321-8505, Japan, ³⁴Polar Studies Division, Geological Survey of India, NHSP, NIT, Faridabad 121001, Haryana, India, ³⁵Department of Geology, Universitet i Tromsø, N-9037 Tromsø, Norway, ³⁶State Key Laboratory of Marine Geology, Tongji University, 1239 Spring Road, Shanghai 200092, China, ³⁷School of Earth Sciences, University of Queensland, St Lucia, Brisbane, Queensland 4072, Australia, ³⁸Earth and Planetary Science, University of Tokyo, 7-3-1 Hongo, Bunkyo-ku, Tokyo 113-0033, Japan.